Multi-Satellite Diversity through the Use of OTFS

Stefano Buzzi[1], Giuseppe Caire[2], Giulio Colavolpe[3], Carmen D'Andrea[1], Tommaso Foggi[3], Amina Piemontese[3], Alessandro Ugolini[3]

[1] University of Cassino and Southern Latium, Italy
[2] Technical University of Berlin, Germany
[3] University of Parma, Italy

Stresa, 21 October 2022

UNIVERSITÀ DI PARMA

Outline

Outline

SPADiC

Motivations

- **LEO satellites** offer an effective way to ensure **global coverage** in B5G non-terrestrial networks
- We consider the use of **multiple LEO satellites** to improve the **spectral efficiency** and increase the **robustness** and **reliability** of the communication link
- **Diversity** can ensure significant gains, but it poses different **challenges**
- Signals received at UTs will have different **delays**, **phases**, and **Doppler shifts**
- **OFDM** does not appear to be an ideal choice in this scenario
- We propose the use of **OTFS**, specifically designed for terrestrial time varying channels

The use of OTFS in non-terrestrial networks has not been considered yet

Outline

Analyzed scenario

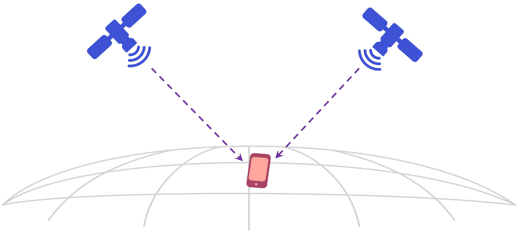

- **Two LEO satellites**
- The **same signal** is transmitted
- UT on the ground
- Different **distance** from the UT
- Different **delays** $\{\tau_p\}_{p=1}^{2}$
- Different **Doppler shifts** $\{\nu_p\}_{p=1}^{2}$

Outline

1. Introduction

2. System model

3. Orthogonal Time Frequency Space (OTFS) Modulation

4. Detection Strategies

5. Numerical Results

6. Conclusions

Orthogonal Time Frequency Space (OTFS) (1/3)

OTFS can be described as follows

- Symbols $\{x[k,l]\}$, $k = 0, 1, \ldots, N-1$, $l = 0, 1, \ldots, M-1$, belonging to any modulation format (e.g., QAM or PSK), **are arranged in an $N \times M$ grid in the Doppler-delay domain**, spaced by $\frac{1}{NT}$ and $\frac{1}{M\Delta f}$
- T and Δf are selected such that

$$\max_p \tau_p < T \,, \quad \max_p \nu_p < \Delta f$$

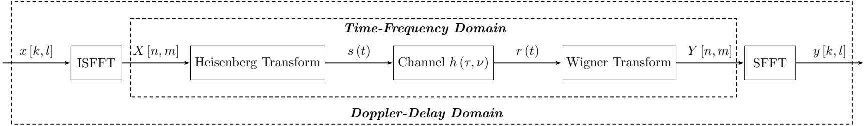

Orthogonal Time Frequency Space (OTFS) (2/3)

- Information symbols are converted into a block of samples $\{X[n,m]\}$ in the time-frequency domain through the **2-D inverse symplectic finite Fourier transform (ISFFT)**

$$X[n,m] = \frac{1}{\sqrt{NM}} \sum_{k=0}^{N-1} \sum_{l=0}^{M-1} x[k,l] e^{j2\pi\left(\frac{nk}{N} - \frac{ml}{M}\right)}$$

- The internal dashed rectangle is nothing else than **a legacy OFDM system**: in fact, the Heisemberg Transform gives the transmitted signal (N OFDM words with M subcarriers)

$$s(t) = \sum_{n=0}^{N-1} \sum_{m=0}^{M-1} X[n,m] g_{\text{tx}}(t - nT) e^{j2\pi m \Delta f t}$$

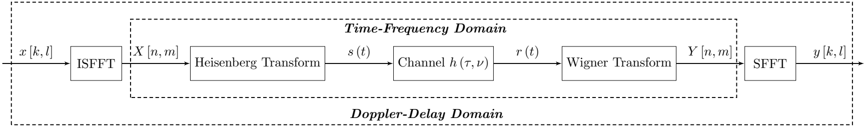

SPADiC

- The cyclic prefix is not necessary (a guard interval of N symbols in the time domain is usually inserted). We will assume $\Delta f T = 1$
- Received signal

$$r(t) = \sum_{p=1}^{P} h_p s(t-\tau_p) e^{j2\pi\nu_p t}$$

- Samples $Y[n,m]$ at the output of a bank of MFs for $t = nT$ and $f = m\Delta f$
- Doppler-delay received samples: $Y[n,m] \xrightarrow{\text{SFFT}} y[k,l]$

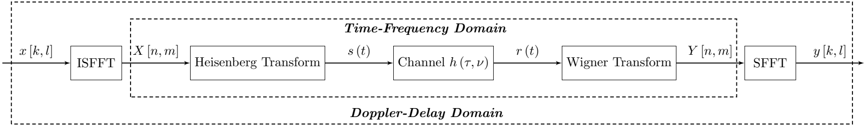

UNIVERSITÀ DI PARMA

Outline

OTFS Detection

SPADiC

- Input-output expression $\boldsymbol{y} = \boldsymbol{\Psi}\boldsymbol{x} + \boldsymbol{w}$: **general model for linear channels**
  - The same model holds for: SC modulations with ISI, OFDM with ICI, MIMO systems, CDMA systems, storage systems with 2D ISI

- Many solutions are available in the literature. In this work, we consider
  - **LMMSE estimator (complexity $\mathcal{O}\left(N^3 M^3\right)$):**

$$\hat{\boldsymbol{x}}_{\text{LMMSE}} = \boldsymbol{\Psi}^{\text{H}} \left(\boldsymbol{\Psi}\boldsymbol{\Psi}^{\text{H}} + \sigma_w^2 \boldsymbol{I}\right)^{-1} \boldsymbol{y}$$

  - **FG/SPA-based detector.** Defining $\boldsymbol{z} \triangleq \boldsymbol{\Psi}^H \boldsymbol{y}$ and $\boldsymbol{G} \triangleq \boldsymbol{\Psi}^H \boldsymbol{\Psi}$, we can develop a message-passing (MP) algorithm with **complexity linear in the number of non-zero elements of matrix G**

Outline

SPADiC

System parameters

SPADiC

First scenario		
Orbital parameters	Satellite 1	Satellite 2
Semi-major axis [m]	7616400	7576300
Eccentricity	0.0011	0.0013
Inclination [°]	87.9888	87.8240
Right Ascension of Ascending Node [°]	114.1692	307.5095
Argument of Periapsis [°]	42.6046	42.7865
True Anomaly [°]	295.8847	42.1175
Period [s]	6615.1	6563
Second scenario		
Orbital parameters	Satellite 1	Satellite 2
Semi-major axis [m]	7594800	7592600
Eccentricity	0.0015	0.0015
Inclination [°]	87.9854	87.9857
Right Ascension of Ascending Node [°]	114.9085	115.0746
Argument of Periapsis [°]	75.4521	65.3493
True Anomaly [°]	343.6983	64.7552
Period [s]	6586.9	6584.1

- **Two scenarios:** comparable and unbalanced channel gains
- **Oneweb** constellation
- Carrier frequency 5 GHz
- Bandwidth 2 MHz
- $M = 128$, $N = 50$
- Subcarrier spacing 15.65 kHz
- Symbol time $66.6\ \mu$s
- QPSK modulation

*The two satellites can perfectly **compensate for delay** at one **reference point** on the surface of the Earth*

Comparable channels, reference point

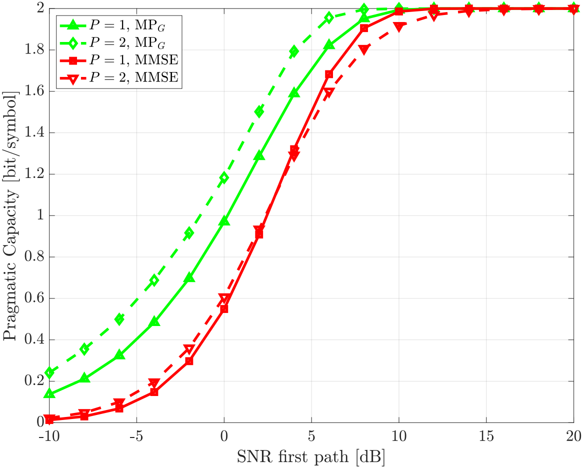

- Comparable channels
- Reference point
- MP_G and $P = 2$ ensure a **significant gain** w.r.t. $P = 1$
- Smaller gains with MMSE

Comparable channels, different positions

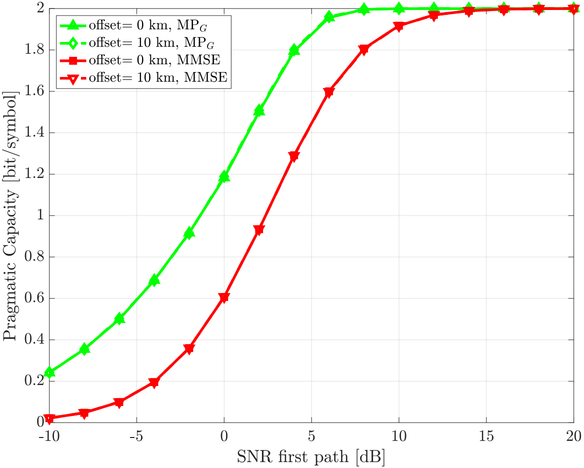

- Comparable channels
- $P = 2$
- Different positions
- The proposed solution is **robust to offset variations**
- The two paths are in both cases different points on the $M \times N$ grid

Comparable channels, shadowing

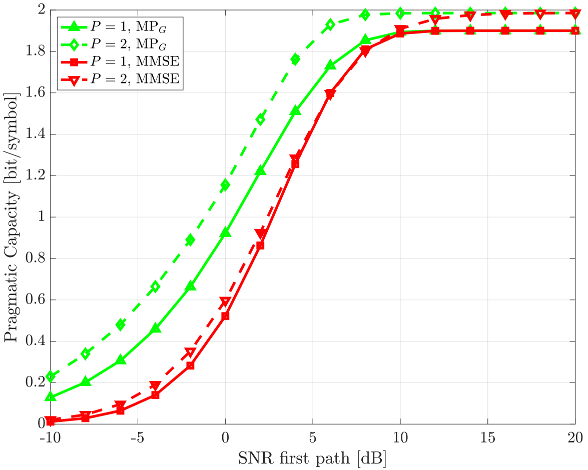

- Comparable channels
- Reference point
- 5% shadowing probability for each path
- Diversity allows a more **robust and reliable link**

Unbalanced channels, reference point

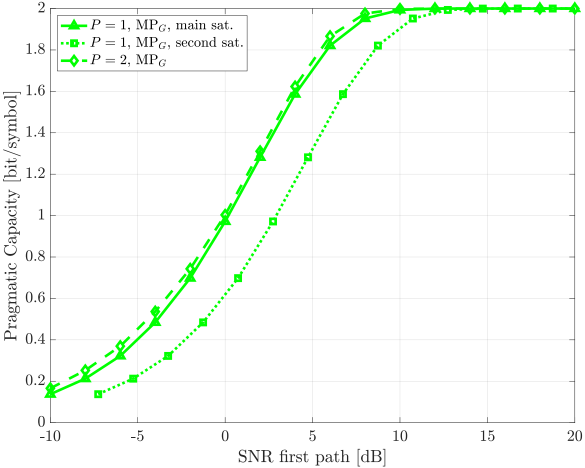

- Unbalanced channels
- Reference point
- MP$_G$ and $P = 2$ ensure a good gain w.r.t. $P = 1$
- especially when the second satellite is used

Unbalanced channels, shadowing

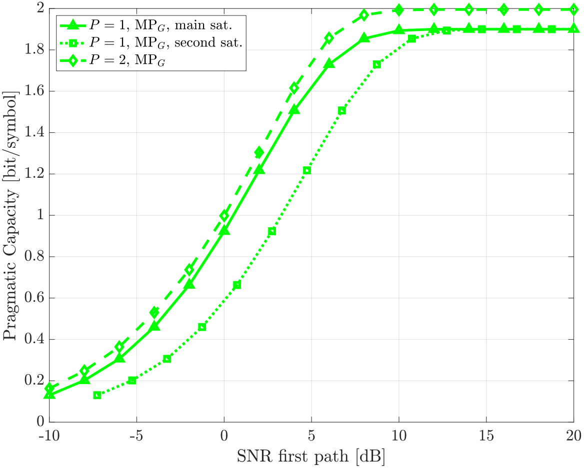

- Unbalaned channels
- Reference point
- 5% shadowing probability for each path
- Diversity allows a more **robust and reliable link**

Outline

Conclusions

- We investigated **diversity techniques** in multiple satellite systems exploiting **OTFS**
- The proposed system ensures
  - **robustness to delay and Doppler shifts** thanks to the properties of OTFS
  - higher **reliability** thanks to the use of diversity
  - higher **achievable information rates** with respect to a single satellite
  - easy **compatibility** with OFDM systems

THANK YOU

Alessandro Ugolini, PhD
SPADiC Lab
Dept. of Engineering and Architecture
University of Parma
alessandro.ugolini@unipr.it

UNIVERSITÀ DI PARMA

www.unipr.it

OTFS: input-output expression (1/3)

- Received samples after SFFT (in the absence of noise):

$$y[k,l] = \sum_{p=1}^{P} \sum_{k'=0}^{N-1} \sum_{l'=0}^{M-1} \underbrace{h_p e^{j2\pi\nu_p\tau_p}}_{h'_p} \boldsymbol{\Psi}^p\left[k,k',l,l'\right] x[k',l']$$

  $y[k,l]$ depends on more symbols $x[k',l'] \Rightarrow$ **Doppler-delay ISI** $\Rightarrow$ **symbol-by-symbol detection is suboptimal**

- When $g_{\text{tx}}(t)$ is a rectangular pulse of support T

$$\boldsymbol{\Psi}^p\left[k,k',l,l'\right] \simeq \frac{1}{NM} \frac{1-e^{j2\pi\left(k'-k+\nu_p NT\right)}}{1-e^{j2\pi\frac{(k'-k+\nu_p NT)}{N}}} \frac{1-e^{j2\pi\left(l'-l+\tau_p M\Delta f\right)}}{1-e^{j2\pi\frac{(l'-l+\tau_p M\Delta f)}{M}}}$$

$$\cdot\, e^{j2\pi\nu_p\frac{l'}{M\Delta f}} \begin{cases} 1 & \text{if } l' \in \left[0, M-1-\lceil\frac{\tau_p}{(T/M)}\rceil\right] \\ e^{-j2\pi\left(\frac{k'}{N}+\nu_p T\right)} & \text{if } l' \in \left[M-\lceil\frac{\tau_p}{(T/M)}\rceil, M-1\right] \end{cases}$$

OTFS: input-output expression (2/3)

- Dirichlet kernel functions:

$$\left|\frac{1-e^{j2\pi\left(k'-k+\nu_p NT\right)}}{1-e^{j2\pi\frac{\left(k'-k+\nu_p NT\right)}{N}}}\cdot\frac{1-e^{j2\pi\left(l'-l+\tau_p M\Delta f\right)}}{1-e^{j2\pi\frac{\left(l'-l+\tau_p M\Delta f\right)}{M}}}\right| =$$

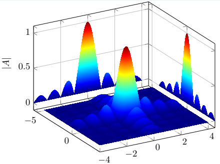

When $P = 1$

- Every symbol is shifted by the same quantity $\propto$ to the Doppler-delay pair associated to the reflector $h\left(\nu,\tau\right)=h_1\delta\left(\tau-\tau_1\right)\delta\left(\nu-\nu_1\right)$
- Leakage in the adjacent positions $\Rightarrow$ Doppler-delay ISI

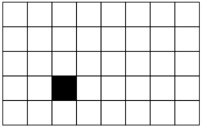

When $P > 1$

- We have P different shifts (P is typically small) $h\left(\nu,\tau\right)=\sum_{p=1}^{P}h_p\delta\left(\tau-\tau_p\right)\delta\left(\nu-\nu_p\right)$

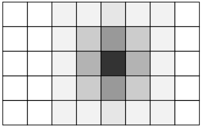

Writing the $N \times M$ matrices of transmitted symbols and received samples as NM-dimensional column vectors (stacking the columns of the corresponding matrices on top of each other), we obtain the block-wise input-output relation as

$$\boldsymbol{y} = \underbrace{\left(\sum_{p=1}^{P} h'_p \boldsymbol{\Psi}_p \right)}_{\boldsymbol{\Psi}} \boldsymbol{x} + \boldsymbol{w}$$

where $\boldsymbol{\Psi}_p$ is the $NM \times NM$ matrix obtained from $\boldsymbol{\Psi}^p [k, k', l, l']$ while $\boldsymbol{w}$ denotes the AWGN with zero mean and covariance $\sigma_w^2 \mathbf{I}_{NM}$.

Dirichlet kernel functions

- Dirichlet kernel functions:

$$\left| \frac{1 - e^{j2\pi\left(k' - k + \nu_p NT\right)}}{1 - e^{j2\pi \frac{\left(k' - k + \nu_p NT\right)}{N}}} \cdot \frac{1 - e^{j2\pi\left(l' - l + \tau_p M \Delta f\right)}}{1 - e^{j2\pi \frac{\left(l' - l + \tau_p M \Delta f\right)}{M}}} \right| =$$